Earth and Planetary Science Letters 519 (2019) 141–151

Contents lists available at ScienceDirect

Earth and Planetary Science Letters

www.elsevier.com/locate/epsl

The effects of back-arc spreading on arc magmatism

Valentina Magni

The Centre for Earth Evolution and Dynamics (CEED), Department of Geosciences, University of Oslo, Sem Sælands vei 2A, Oslo, Norway

ARTICLE INFO

Article history:
Received 24 September 2018
Received in revised form 3 May 2019
Accepted 6 May 2019
Available online xxxx
Editor: R. Bendick

Keywords:
subduction
back-arc
arc magmatism
mantle flow
numerical models

ABSTRACT

Mantle flow is a key feature that can affect melt production and composition in and around subduction zones. In this study, I use three-dimensional numerical models to investigate the role of mantle flow on subduction-related volcanism during back-arc extension. Results show that for a time interval of about 10-15 Myr during back-arc basin formation and spreading a wide convection cell brings mantle that has already partially depleted at the back-arc to the mantle wedge. Before and after this phase, the mantle reaching the sub-arc melting region is fertile. Thus, changes in back-arc activity and mantle flow pattern can be responsible for changes in magmatic composition and the amount of magmatism at the arc. These results are consistent with many examples of present-day subduction zones, in which phases of actively spreading back-arc correspond to a gap or a decrease of the arc volcanic activity.

1. Introduction

Magmatism associated with subduction zones takes place not only at arcs but also at back-arcs and along transform faults at the edges of retreating trenches. Arcs are arguably the most studied for various reasons; they are a feature of every oceanic subduction setting, they are often characterized by highly hazardous explosive volcanoes due to the high volatile contents of their magmas, and they are the places where most of the continental crust is generated (e.g., Ringwood, 1974). On the other hand, magmatism at the back-arc and at the Subduction-Transform Edge Propagator (STEP) faults (Govers and Wortel, 2005) is not always present in subduction settings and differs from the arc-type in terms of composition and physical properties. Although distinct, these three types of magmatism belong to the same regional tectonic setting and they all respond and evolve accordingly to the dynamics of subduction. To fully understand them, it is therefore important to take into account the large spatial and temporal scales in which they operate. It is also crucial to investigate if and how they interact with each other and how they are affected by changes in subduction dynamics and associated mantle flow.

Magmatic activity at the back-arc can occur in oceanic subduction settings when the overriding plate is under extension (Uyeda and Kanamori, 1979). The thinning of the lithosphere due to extensional stresses allows the mantle to rise to shallow depths and melt through adiabatic decompression, creating new oceanic crust in a process similar to spreading at mid-ocean ridges. If the spreading centre is close to the arc, fluids released from the downgoing slab can reach the melting zone beneath the ridge (Hawkins and Melchior, 1985). Indeed, geochemical studies show that back-arc magmas have a subduction signature in their trace elements and water content, which is stronger with the proximity to the arc (Pearce and Stern, 2006). This is also in agreement with geophysical studies that find distinct types of oceanic crust formed at different distances between the arc and the spreading centre; a thicker and more differentiated crust forming close to the arc is interpreted to be a consequence of higher water content (Arai and Dunn, 2014). Many studies have shown the effect of slab fluids on back-arc magmatism (Arai and Dunn, 2014; Hawkins and Melchior, 1985; Harmon and Blackman, 2010); however, there has been less focus on the effect of an actively spreading back-arc on the volcanic activity at the arc. The composition and amount of arc magmatism depends on several factors, such as the slab dehydration pattern, composition of the subducting plate, thermal structure of the subduction zone, mantle wedge dynamics, mantle source and melt migration, thickness and composition of the overriding plate, fractional crystallization processes, and overriding plate stresses (Arculus and Powell, 1986; Ducea et al., 2015; Magni et al., 2014a; Pearce and Peate, 1995). Woodhead et al. (1993) suggested that the magmatic activity of the back-arc basin affects that at the arc because mantle flow can bring mantle that has experienced melting at the back-arc to the sub-arc region. Cooper et al. (2010) interpreted the presence of high-Ca boninites in the Tonga arc as the result of melting of an already depleted mantle source coming from the actively spreading Lau Basin. Numerical models by Hall et al. (2012) predict an increasingly depleted mantle source beneath the arc following the

E-mail address: valentina.magni@geo.uio.no.

https://doi.org/10.1016/j.epsl.2019.05.009

onset of spreading. However, these are kinematic models that do not take into account the changes in subduction dynamics, such as changes in plates and trench velocity, and the complexity derived from the three-dimensionality of the system.

Back-arc basins formation is a particularly 3D process as it often happens adjacent to collision of a buoyant feature (e.g., continent, oceanic plateau, and seamount chain), which locally slows down or ceases subduction and triggers fast trench retreat and rotation next to it (Magni et al., 2014b; Wallace et al., 2009). In some scenarios, back-arc extension occurs without rotation simply due to the fast retreating velocity of the narrow slab (e.g., East Scotia Basin), or because the overriding plate moves away from the trench (e.g., Marianas). In any case, the dynamics of the neighbouring plates and the 3D geometry of the subduction zone have a significant control on the formation of back-arc basins. Moreover, slab break-off and tearing can occur adjacent to the ongoing oceanic subduction where the back-arc is rifting or spreading, forming slab windows that allow the mantle to flow in a toroidal fashion (Magni et al., 2014b). In the Tyrrhenian basin, it has been suggested that the mantle flowing through the slab window beneath the African margin has affected the back-arc magmatism, changing its composition from calc-alkaline to alkaline (Faccenna et al., 2005). Mantle flow is, thus, a key feature that influences volcanism in subduction zones. Importantly, previous numerical models that studied the link between arc and back-arc are mostly two-dimensional and kinematic (e.g., Hall et al., 2012; Harmon and Blackman, 2010), whereas those that looked at back-arc basins formation in 3D did not focus on the mantle flow and source of magmatism (Hashima et al., 2008; Moresi et al., 2014). Here I use 3D fully dynamic models of subduction to study the mantle source of arc and back-arc melts during the evolution of back-arc spreading and trench retreat.

2. Methods

The main aim of this study is to investigate the time-dependence of mantle flow and melt production in a subduction setting in which the overriding plate is under extension and spreading occurs at the back-arc. Wallace et al. (2009) showed that rifting in most back-arcs is associated with rapid rotation of the fore-arcs, which is caused by adjacent collision of buoyant indentors. Therefore, here I use similar models to those developed in Magni et al. (2014b), in which the formation of back-arc basins is a consequence of nearby continental collision. Subduction of oceanic and continental lithosphere in the upper mantle is modelled using the finite element code CITCOM (Moresi and Gurnis, 1996). The code solves for conservation of mass, momentum, energy, and composition in a Cartesian geometry, assuming incompressible flow and adopting the Boussinesq approximations (symbols in Table 1):

$$\nabla \cdot u = 0$$

$$-\nabla P + \nabla \cdot \left(\eta\left(\nabla u + \nabla^T u\right)\right) + (Ra_T + Ra_C)e_z = 0$$

$$\frac{\partial T}{\partial t} + u \cdot \nabla \mathrm{T} = \nabla^2 T$$

$$\frac{\partial C}{\partial t} + u \cdot \nabla \mathrm{C} = 0$$

Where Ra_T is the thermal Rayleigh number:

$$Ra_T = \frac{\alpha \rho_0 g \Delta T h^3}{k \eta_0}$$

And Ra_C is the compositional Rayleigh number that takes into account the different buoyancy of the continental crust:

Table 1
Symbols and units of the used parameters.

Parameters	Symbols	Value and unit
Rheological pre-exponent	A	6.52×10^6 [$\mathrm{Pa}^{-n}\,\mathrm{s}^{-1}$]
Activation energy	E	360 [kJ/mol]
Vertical unit vector	e_z	[-]
Gravitational acceleration	g	9.8 [$\mathrm{m/s^2}$]
Box height	h	660×10^3 [m]
Rheological power law exponent	n	1 (diff. c.), 3.5 (disl. c.) [-]
Lithostatic pressure	p_0	[Pa]
Deviatoric pressure	P	[Pa]
Gas constant	R	8.3 [J/K/mol]
Absolute temperature	T_{abs}	[K]
Reference temperature	T_m	1350 [°C]
Time	t	[s]
Velocity	u	[m/s]
Thermal expansion coefficient	α	3.5×10^{-5} [K^{-1}]
Compositional density contrast	$\Delta\rho_c$	600 [$\mathrm{kg/m^3}$]
Second invariant of the strain rate	$\dot{\varepsilon}_{\mathrm{II}}$	[s^{-1}]
Effective viscosity	η	[Pa s]
Reference viscosity	η_0	10^{20} [Pa s]
Maximum lithosphere viscosity	η_{max}	10^{23} [Pa s]
Friction coefficient	μ	0.1 [-]
Thermal diffusivity	k	10^{-6} [$\mathrm{m^2/s}$]
Reference density	ρ_0	3300 [$\mathrm{kg/m^3}$]
Yield stress	τ_y	[MPa]
Surface yield stress	τ_0	40 [MPa]
Maximum yield stress	τ_{max}	400 [MPa]
Continental crust thickness	Hc	40 [km]

$$Ra_C = \frac{\Delta \rho_c g h^3}{k \eta_0}$$

Passive tracers are used to track the compositional information (continental crust material, water content, and depletion) and are advected with the velocity field.

The size of the computational domain is $3300 \times 3960 \times 660$ km and the finite mesh size varies from $20 \times 20 \times 20$ km to $8 \times 8 \times 8$ km, with the smallest elements located in the trench region where the highest resolution is required due to large viscosity contrasts. The initial geometry includes a slab down to 250 km depth in order to initiate subduction (Fig. 1). The slab sinks into the mantle due solely to its negative buoyancy; no other forces are applied to the plates. The subducting plate is comprised of a central domain of oceanic lithosphere with two continental blocks at the side, whereas the overriding plate is fully continental (Fig. 1a). Initially, subduction of oceanic lithosphere takes place everywhere along the trench, then, continental collision occurs at the sides and oceanic subduction continues in the middle. I run an additional model with the opposite geometry of the subducting plate (i.e., continental lithosphere in the middle and oceanic lithosphere at the sides) to investigate different types of toroidal mantle flow (Fig. 1b). These types of setup produce localised fast trench retreat, which results in back-arc basins formation. Although this is not the only way to produce back-arc spreading, it is a common one (Wallace et al., 2009) and these model setups allow to focus on the study of the mantle flow during trench retreat and back-arc extension, regardless of what the causes of trench retreat are.

For the oceanic lithosphere, the initial temperature field follows the half-space cooling model for an 80 Myr old plate (Turcotte and Schubert, 2002). In the continental parts, temperature linearly increases from 0 °C at the surface to 1350 °C, which is the mantle reference temperature, at a depth of 150 km. The temperature boundary conditions are the following: fixed values at the surface (0 °C), at the bottom and on the left hand-side (1350 °C), and zero heat flux in all the other boundaries. Velocity boundary conditions are no slip at the bottom to simulate the high viscosity contrast between upper and lower mantle, and free slip everywhere else.

To allow the mantle to flow around the edges of the slab, the width of the subducting and overriding plates is smaller than the

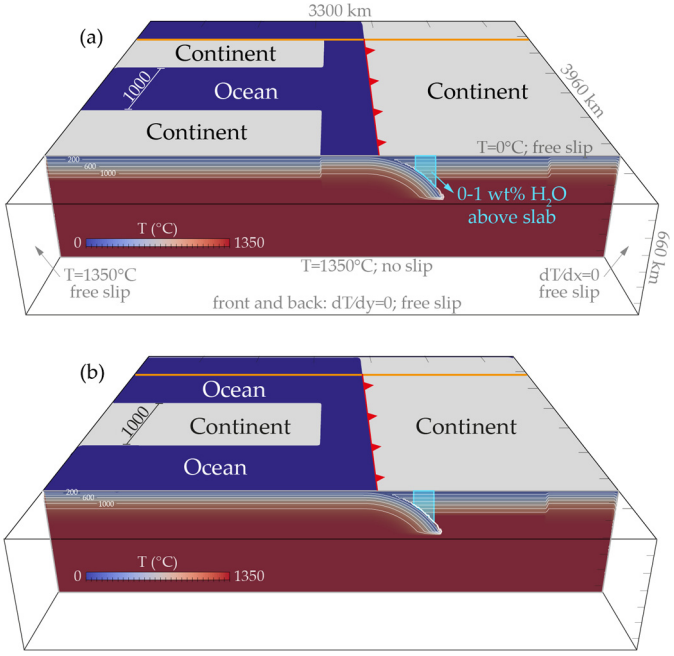

Fig. 1. Initial model setup, thermal structure, and boundary conditions. Continental and oceanic lithosphere are showed in grey and blue, respectively. The light blue area above the slab shows the hydrated region as defined in Methods. Trench position is marked by the red line with triangles on the overriding plate. The orange line shows the position of one of the transform faults (at $y = 660$ and 3300 km) that decouple the plates from the rest of the lithosphere. (For interpretation of the colours in the figure(s), the reader is referred to the web version of this article.)

width of the computational domain. This is modelled by imposing two narrow (20 km) low viscosity (10^{20} Pa s) zones that simulate transform faults and decouple the plates from the rest of the lithosphere. Subduction is enabled by a 20 km wide low viscosity zone (10^{20} Pa s) between the plates to a depth of 50 km. Below this depth, above the slab, the mantle wedge has also the reference mantle viscosity to simulate the weakening effects of fluids and melt present in the wedge. In the rest of the domain, mantle and lithosphere have a stress and temperature dependent viscosity, following the power law (Hirth and Kohlstedt, 2003; Korenaga and Karato, 2008):

$$\eta = A\dot{\varepsilon}_{\mathrm{II}}^{\frac{1-n}{n}} exp\left(\frac{E}{nRT_{abs}}\right)$$

Where $n = 1$ for diffusion creep and $n = 3.5$ for dislocation creep. Additionally, the viscosity due to yielding is computed as follows (Byerlee, 1978):

$$\eta = \frac{\tau_y}{\dot{\varepsilon}_{\mathrm{II}}} \qquad \tau_y = min(\tau_0 + \mu p_0, \tau_{max})$$

At each node of the finite grid, viscosity values of the above mechanisms are computed and the effective viscosity is the lowest value among them.

2.1. Mantle wedge hydration and melting

To compute the melt fraction as a function of pressure, temperature, and water content I use the parameterization of hydrous mantle melting of Katz et al. (2003). The mantle wedge above the slab is continuously hydrated up to 200 km depth to simulate the dehydration of the subducting plate. The wedge water content is varied in different models from 0 to 1 wt% to explore the effect of water on flux melting and arc magmatism. The amount of depletion is stored in the passive tracers and this information is utilized to discern if a tracer is able to melt further. For example, if a tracer is already 10% depleted and reaches PT conditions in which the melt at equilibrium is <10%, then no additional melt will be produced. Moreover, if melting occurs, water content is updated accordingly, following the parameterization of Katz et al. (2003). Finally, I use the tracer position and depletion amount to analyse the mantle flow and investigate where the mantle that experiences melting comes from, and whether it is already partially depleted or is still fertile when it reaches the melting regions at the arc and/or at the back-arc.

3. Results

In this study, I perform a series of 3D models aimed at investigating the role of the mantle flow on arc and back-arc magmatism. I first describe the results of the reference model that has the initial setup showed in Fig. 1a and the models with the same geometry but with different water contents in the mantle wedge. Next, I compare these results with a model that has a narrower (700 km instead of 1000 km) central oceanic region and in which the dynamics changes because slab tear does not occur (Magni et al., 2014b). Finally, I show results of the model with the opposite geometry of the subducting plate compared to the reference model (Fig. 1b).

3.1. Reference model

3.1.1. Subduction dynamics

In all models presented in this study subduction starts with an oceanic lithosphere entering the trench and, only after the slab has reached the bottom of the box (660 km), the continental part of the subducting plate enters the trench and collides with the overriding plate. In the reference model, collision occurs at the sides of the plate, whereas the subducting plate is still oceanic in the middle (Fig. 2; Supplementary Material A1). This along-trench variation in thickness, composition and buoyancy of the subducting plate causes the trench to migrate in different ways. At the sides, where continental collision occurs, subduction drastically slows down and the trench slightly advances until the slab breaks off due to the positive buoyancy of the continental crust that opposes subduction. In the middle, however, oceanic subduction is ongoing and the retreat of the slab accelerates, going from 2 cm/yr to 5.5 cm/yr in only a few Myrs (Fig. S1a). This causes extension in the overriding plate and leads to the formation of a back-arc basin. At its peak velocity, right after the formation of the back-arc basin, a full spreading rate of ~6 cm/yr is observed. The spreading rate is approximately uniform along the y-direction, with only slightly smaller values at the side of the basin. The oceanic slab continues to retreat, tearing at depth along the ocean-continent boundaries and forming two slab windows (Fig. 2d-e).

3.1.2. Melting at the arc and back-arc

During oceanic subduction, the mantle wedge above the slab is hydrated with 1% water leading to melt production. With the thinning of the overriding plate due to extension, temperatures in the mantle wedge increase, causing higher melt production. Indeed, the degree of depletion in the mantle wedge reaches a peak of 28% (Fig. 3). Before the back-arc basin forms, at about 18 Myr since the beginning of the model (i.e., since its initial setup), the mantle melts only above the slab, in the sub-arc region (Fig. 3a). However, when the back-arc basin forms, the overriding plate gets thin enough that adiabatic decompression melting occurs. At the initial stage, back-arc spreading commences only 50 km away from the arc and the two melting regions, at the arc and back-arc, are connected to each other (Fig. 3b). Therefore, melts at the back-arc might be affected by fluids released from the slab, and thus be

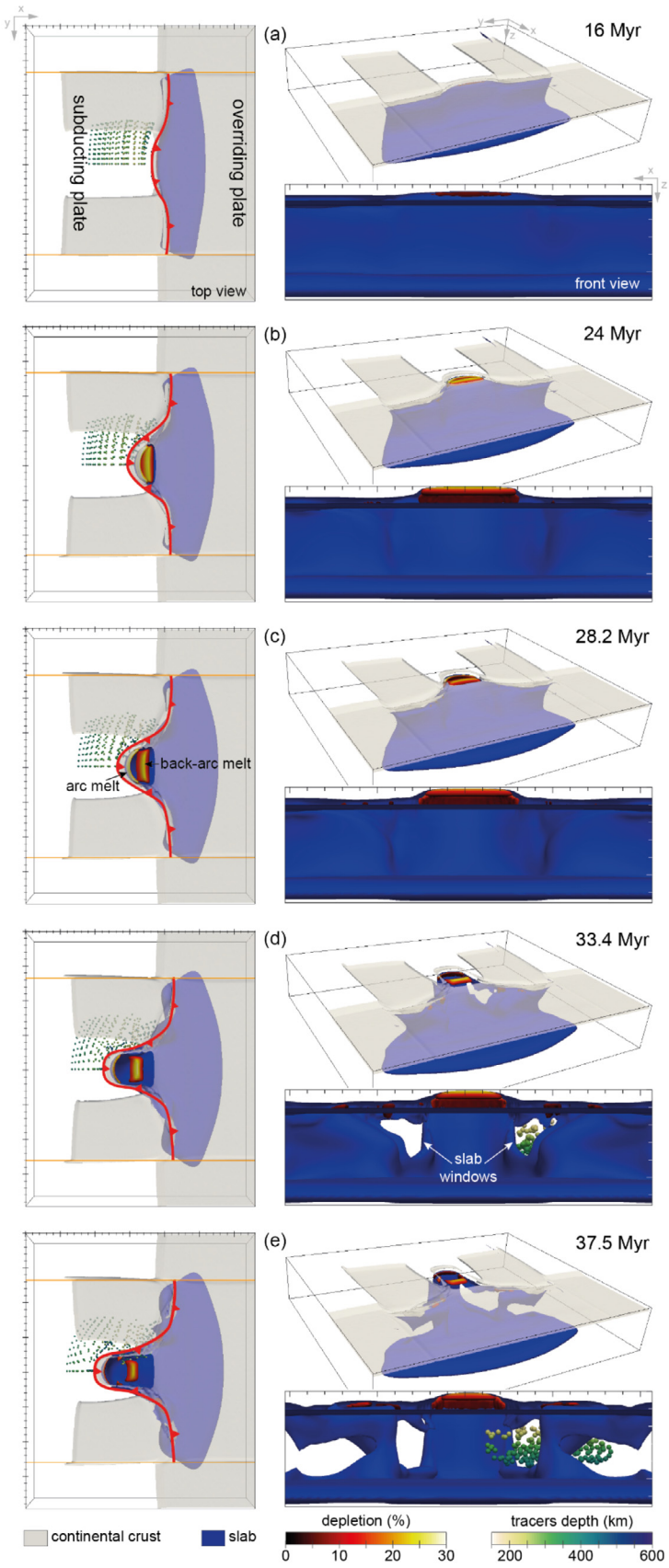

Fig. 2. Reference model dynamics: after collision at the sides of the central oceanic domain occurs (a), the trench starts to rapidly retreat in the middle triggering back-arc spreading (b-e) and eventually slab windows formation at depths (d-e). The contour in the red-to-white colour map indicates the regions of melt at equilibrium and the amount of melt fraction. Continental crust is showed in grey. The isosurface of $T = 1080\,^{\circ}\mathrm{C}$ shows the subducting lithosphere. Passive tracers colour-coded by depth show the toroidal mantle flow. Trench position is marked by the red line with triangles on the overriding plate. Orange lines show the position of the transform faults. Full dynamics in Supplementary Material animation A1.

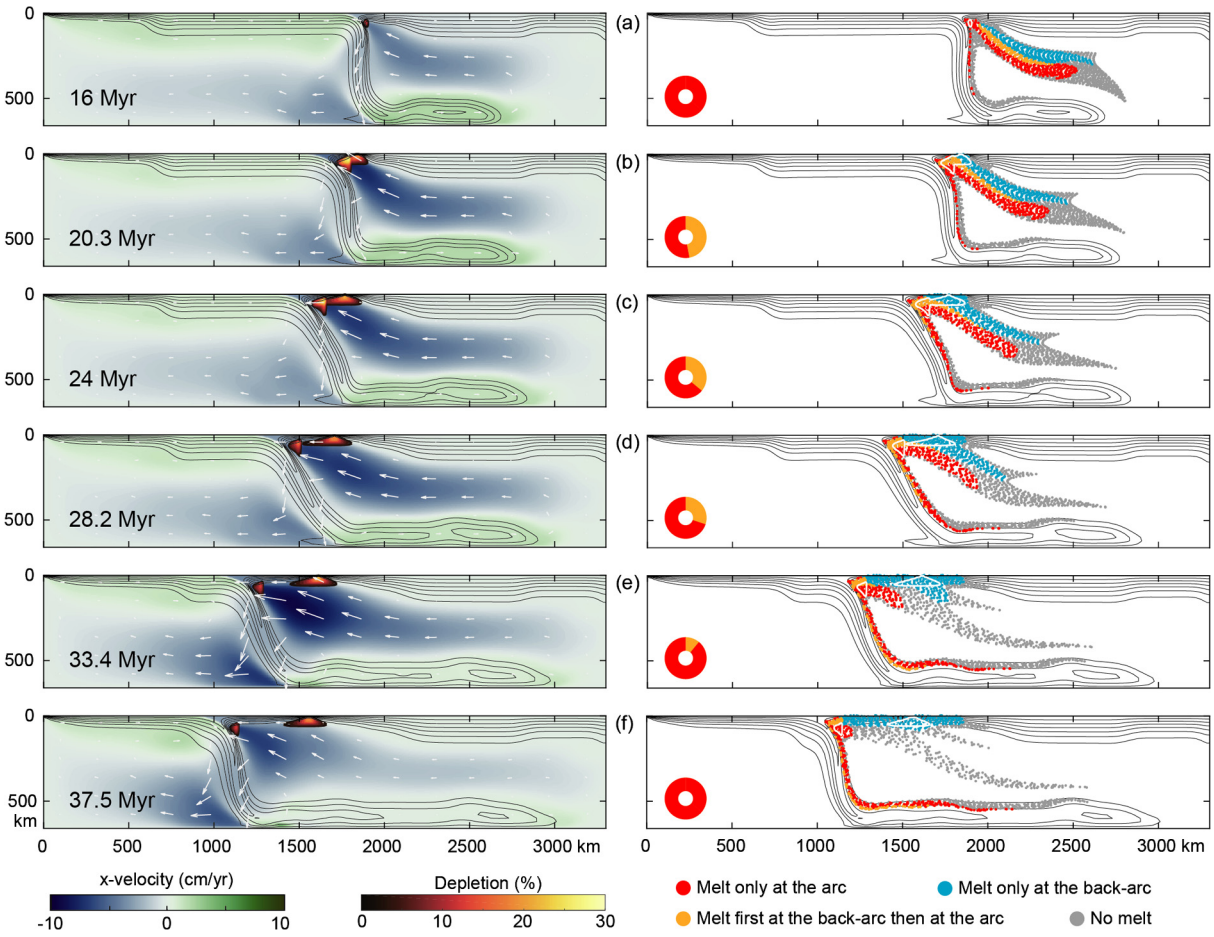

Fig. 3. Mantle flow and melting across a vertical section in the middle of the domain (oceanic subduction) of the reference model. The left column shows the horizontal velocities and the melt at equilibrium beneath the arc and back-arc. On the right, mantle flow is shown with tracers for the same time steps. Different tracer colours distinguish between tracers that never melt (grey), those that melt only at the back-arc (light blue), only at the arc (red), or first at the back-arc and then at the arc (yellow). White contour of 0.03 melt fraction (or 3% depletion) shows the regions of equilibrium melt. The doughnut charts at the bottom left corners indicate the percentage of already depleted material coming from the back-arc (in yellow) in the mantle wedge within the sub-arc melting region. Thus, when the doughnut chart is entirely red the source of melting is fertile mantle. Isotherms, in grey, are shown every 200 °C. Perceptually uniform colour maps from www.fabiocrameri.ch are used to prevent visual distortion of data.

a combination of subduction-related melts and adiabatic decompression melting. As the trench keeps retreating, the arc and the back-arc melting regions become further apart until they are not connected any longer and the back-arc melts are not affected anymore by subduction fluids (Fig. 3d). A second pulse of higher melt production at the back-arc is observed during the second pulse of fast trench retreat, when the slab windows form.

3.1.3. Mantle flow and melting

Firstly, I describe the mantle flow in a 2D vertical section in the middle of the subducting plate, which represents a symmetry plane and therefore it is not directly affected by the 3D flow and, secondly, the 3D toroidal flow. During the initial stages, the subducting plate is driving the corner flow in the mantle wedge: fertile mantle material flows below the arc and is then dragged down by the subducting slab (Fig. 3a). When the back-arc basin forms, this 'corner flow' cell widens; the mantle first ascends to the back-arc region and then reaches the mantle wedge (Fig. 3b-e). Therefore, although the melting regions at this point are only slightly connected or not connected at all, they still interact with each other because of the mantle flow pattern. Indeed, the mantle that flows beneath the arc comes from the back-arc region where it has been partially depleted. This can be observed even better by tracking passive tracers in this vertical section during the model evolution. Fig. 4a shows where these tracers are when they reach the peak of depletion. In this way, I can distinguish among tracers that melt only at the back-arc, only at the arc, and, in the case of two peaks of melting, tracers that melt first at the back-arc and then again at the arc. From the moment spreading starts at the back-arc and until ~15 Myr some tracers melt first below the back-arc and then, a few million years after, they reach the arc region. Especially in the first 5 Myr, 30-50% of the mantle source of arc magmatism is already partially depleted (up to 20% depletion) as it comes from the back-arc melting region (Fig. 4).

Looking at the 3D mantle flow, it is interesting to see if the mantle that flows through the slab windows is involved in any type of melting. In this model, this is not the case. The slab breaks off at a depth of ~200 km and the toroidal flow is happening at deeper depths (Fig. 3; Supplementary Material A1). Although there is an upwelling component in the toroidal flow, it is insufficient to bring this mantle material into the melting regions of the back-arc or the arc. In fact, when this mantle material arrives in front of the slab, it is dragged downwards by the corner flow produced by the descending slab.

3.2. Effect of water content

To investigate the effect of water released from the slab on melt production during subduction two additional models are presented; in the first, the amount of water in the mantle wedge is one order of magnitude less than in the reference model (0.1 wt% instead of 1 wt%) and in the second, there is no water released

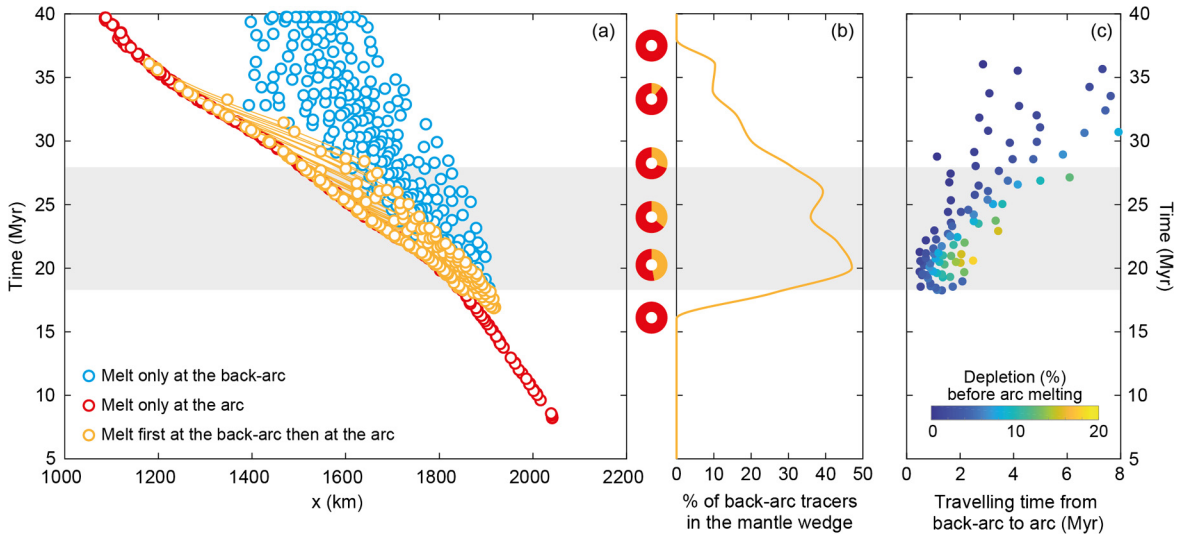

Fig. 4. (a) X-coordinates of the tracers when each reaches the peak of melt at the arc (red) or at the back-arc (light blue). Position of both peaks, for tracers that melt first at the back-arc and then at the arc (yellow). (b) Percentage of already depleted material coming from the back-arc in the mantle wedge. Doughnut chart are the same of Fig. 3. (c) Travelling time from back-arc to arc for the yellow tracers. Colour scale shows their amount of depletion just before they reach the mantle wedge. The grey area shows the interval at which more than 30% of the tracers in the mantle wedge melting region are depleted tracers coming from the back-arc.

into the mantle wedge (Fig. 5). Mantle melting in the model with 0.1 wt% of water is similar to that of the reference model, with a first stage in which the arc and back-arc melting regions are close and interact to each other and a later stage when the trench and the spreading region are far away and not connected anymore (Fig. 5b). As expected, however, a smaller amount of water produces less amount of melt in the mantle wedge (only up to 12% melting, as opposed to a maximum of almost 30% in the reference model). The amount of melt produced at the back-arc is similar to the reference model, whereas melt at the arc is consistently less throughout the entire model. If no water is released from the slab, melting does not occur in the mantle wedge and no arc volcanism would form (Fig. 5c). This is an end-member case to emphasize the importance of slab dehydration on subduction-related volcanism. Slightly more melt is initially produced beneath the back-arc region because there is no distinction between arc and back-arc melts. Afterwards, melt production at the back-arc has a similar pattern and amount than the reference model.

3.3. *Effect of retreating trench velocity decrease*

The dynamics of the model with a narrower oceanic subducting plate is similar to the reference model, with fast trench retreat at the centre after collision at the sides, and the consequent opening of the back-arc basin (see Supplementary Material A2). However, the main difference from the reference model is that slab windows at the ocean-continent boundaries do not form. Because the total slab pull is less than that of the reference model, the trench retreats less and the slab does not deform enough to tear at depth. Therefore, in this case the trench retreating velocity gradually decreases (from 4 cm/yr to <1 cm/yr) and no second pulse of higher melt production is observed at the back-arc. Instead, the overriding plate thickens as it cools, thus the amount of mantle material that reaches the conditions for adiabatic decompression melting progressively decreases until no melt is produced at the back-arc (Fig. 5d).

3.4. *Rotation induced back-arc spreading*

Fig. 6 shows the numerical results of a model with the opposite geometry of the previous experiments, with a continental indenter in the middle of the subducting plate and oceanic lithosphere at its sides (Fig. 1b). This is to explore the effect of a toroidal flow that does not go through slab windows, but instead goes around the edges of the slab. In this case, the cessation of subduction and slab break-off occurs in the middle of the plate. At the sides, oceanic lithosphere continues to subduct and the trench retreats much faster on the slab edge side than closer to the continent (Fig. 6; Supplementary Material A3). Thus, the slab rotates with the corners of the indenter at the trench working as pivot points. Extension at the back-arc is therefore larger the further away from the continent and it progressively decreases towards the pivot point of rotation. The full spreading rate at the back-arc spreading centre reaches peaks of almost 7 cm/yr where the larger rotation occurs and gradually decreases, up to 2.5 cm/yr, closer to the continental block (Fig. S1b). Consequently, melt production is also higher close to the slab edge and it decreases until only rifting is observed close to the continent.

During rotation and retreat of the oceanic slab, the mantle flows from behind to the front of the slab in a toroidal fashion around the slab edge. Interestingly, this flow has a strong upwelling component that brings the mantle towards the surface, at the back-arc and arc regions. Moreover, part of the upwelling mantle flows into the transform fault, which is modelled as a narrow strip that decouples the subducting and overriding plates from the rest of the lithosphere allowing them to move freely (see Methods). Therefore, adiabatic decompression melting not only occurs at the spreading centre of the back-arc basin, but also along the transform fault. Although the mantle flow pattern is different from that of the reference model, there is an important similarity between the two models; a phase of $\sim$10 Myr in which the mantle that melts below the back-arc flows into the mantle wedge region and is part of the mantle source of arc magmatism.

4. Discussion

The mantle flow pattern and melt production during the formation and spreading of a back-arc basin are not steady-state, changing through time as subduction evolves. In this study, I analyse scenarios in which the overriding plate is under extension due to trench retreat. The evolution of this type of system is schematically summarized in Fig. 7. During subduction, the sinking of the slab creates a corner flow that brings fertile mantle into the mantle wedge (McKenzie, 1969) (Fig. 7a). This mantle is the source of arc

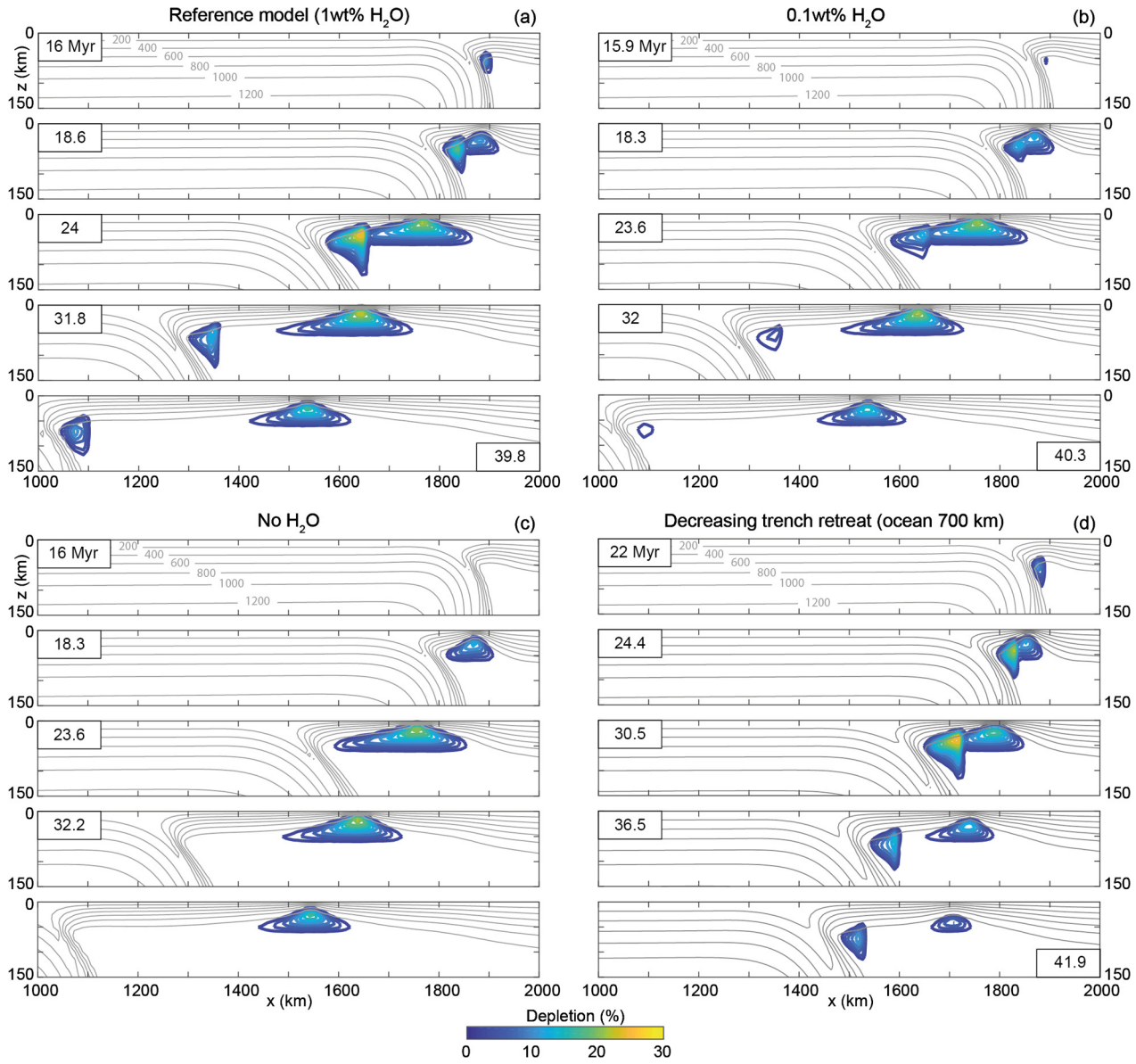

Fig. 5. Evolution of mantle melting at arc and back-arc in a vertical section in the middle of the domain for different models: (a) reference model, with 1 wt% H_2O mantle wedge hydration, (b) model with 0.1 wt% H_2O mantle wedge hydration, (c) no hydration in the mantle wedge, and (d) model with a narrower oceanic plate (700 km) in which the trench velocity decreases after the back-arc basin formation and, thus, the trench retreats less compared to the reference model (full dynamics of this model in Supplementary Material animation A2). Isotherms, in grey, are shown every 200 °C.

magmas, as the fluids released from the slab lower its solidus and trigger melting (Ringwood, 1974; Sobolev and Chaussidon, 1996). Before the back-arc basin forms, this is the only type of melt generated in the system. However, when the trench retreat accelerates, the overriding plate thins and the back-arc basin starts to spread. The melt produced at the back-arc is generated by adiabatic decompression melting of fertile mantle that is upwelling beneath it, similar to mid-ocean ridges (e.g., Kelemen et al., 1997). However, in the initial stage of its formation, the back-arc basin is close to the arc and the two melting regions are connected to each other (Fig. 7b). Therefore, it is reasonable to expect that slab dehydration affects both the arc and the back-arc melts. This is in agreement with many geochemical studies that found signatures of subduction fluids in back-arc lavas (Kelley et al., 2006; Langmuir et al., 2006; Pearce and Stern, 2006). As the trench keeps retreating, the arc and the back-arc spreading centre get further apart (Fig. 7c). Although fluid migration is not explicitly modelled here, it is likely that at this point slab fluids would not affect the melts produced at the back-arc any longer. Geophysical studies in the Lau basin suggest that this happens when the distance between arc and back-arc spreading centre is >70 km (Arai and Dunn, 2014), which is in agreement with the presented models. Interestingly, at this stage, the mantle flow driven by the downgoing slab is no longer the classic corner flow that brings fertile mantle directly in the wedge, but rather is a wider convection cell that brings mantle first below the back-arc region and then below the arc. This type of behaviour has important consequences on the amount and style of arc magmatism because its source changes drastically. Indeed, the mantle that flows into the mantle wedge is already depleted because it has previously melted at the back-arc. My results show that the amount of depleted mantle reaching the mantle wedge during this phase can be up to almost 50% of the total material in equilibrium with the melt below the arc. If such a large amount of mantle above the slab is already depleted by 5-20%, a decrease in the amount of melt generated in the mantle wedge and/or a change in melt composition is expected to occur,

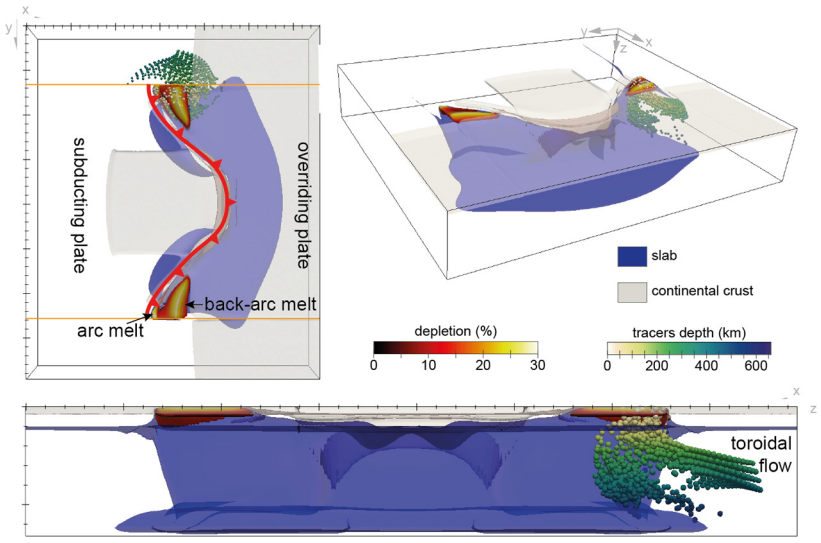

Fig. 6. Snapshots of model c1000 (full dynamics in Supplementary Material animation A3) that has continental block in the middle of the subducting plate and oceanic lithosphere at the sides (setup in Fig. 1b). The strong rotation of the oceanic sides enable the toroidal flow around the slab edge to rise at the surface. See Fig. 2 caption for details on the colour legend.

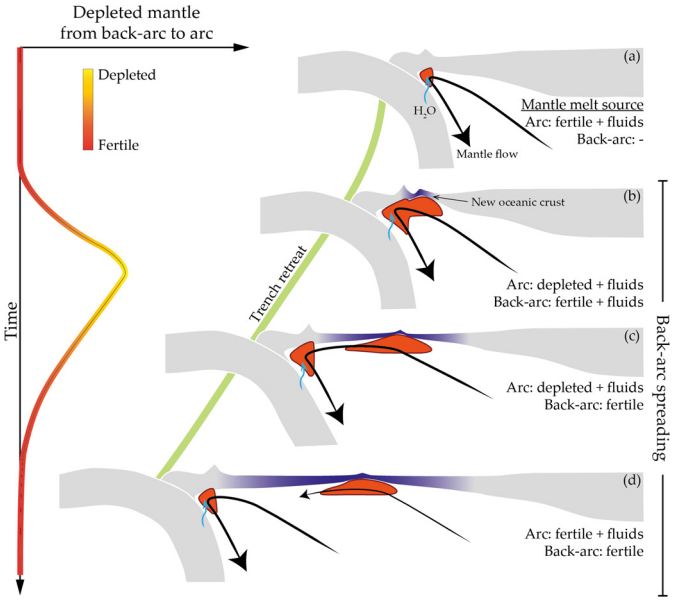

Fig. 7. Schematic cartoon showing the evolution of mantle flow during back-arc spreading and the consequent evolution of the mantle source at the arc (on the left). First, corner flow created by the downgoing slab brings fertile mantle to the mantle wedge (a). Then, back-arc spreading starts close to the arc (b) and as the trench retreats the convection cell of the mantle flow gets wider, bringing depleted mantle from the back-arc to the mantle wedge beneath the arc (c). Finally, the back-arc spreading centre is too far away from the arc to affect its mantle source, which is again fertile mantle brought by the corner flow (d).

since the source of melt is not as fertile as before. This would likely be reflected in the arc volcanic activity and composition (a comparison with natural cases is discussed in 4.2). This type of convection cell lasts ~10-15 Myrs, until the back-arc spreading centre is far away from the trench and the classic corner flow that brings fertile mantle to the wedge below the arc is restored (Fig. 7d).

The transport of depleted mantle from the back-arc to the arc is consistent with previous studies that used geochemical data to investigate the source of melting in arc lavas. Woodhead et al. (1993), for instance, found that melt extraction prior to arc magma genesis explains the trace element pattern observed in island arc basalts and suggested that this extraction might happen at the back-arc. This is also in agreement with the conceptual model used by Cooper et al. (2010) that explains the presence of high-Ca boninites in the Tonga arc with residual peridotite being brought by the mantle flow from the back-arc to the arc mantle wedge. Moreover, Pearce and Peate (1995) showed that the volcanic arc magmas with no back-arc basins exhibit MORB-like or enriched sources.

This study demonstrates that a spreading back-arc during trench retreat can have a key role in arc volcanism because it can affect the type of mantle source of arc melts. The temporary inflow of depleted mantle coming from the back-arc into the mantle wedge has to be taken into account when studying temporal variations in arc magmas. In the presented models, spreading at the back-arc can occur with pulses of higher melt production, but it is continuous. Overall, there is only one phase of mantle wedge melts with a depleted source coming from the back-arc. However, in a more complex system, with alternating episodes of spreading and rifting, the mantle source of arc melts will vary. If derived from the back-arc region, the melt might be depleted if 'sampled' during a spreading phase. Alternatively, the source of arc melts may be fertile if the mantle flows beneath the back-arc during a period of rifting, in which melt is not produced. In this scenario, the signature in arc magmatism would also be more complex and might present alternating phases of depleted and fertile mantle source within only a few millions of years. Moreover, lateral variations within the back-arc basin can add further complexities because spreading and rifting can occur at the same time in different areas. Therefore, the geometry of active spreading centres in a back-arc basin can produce along-trench variations of the amount and composition of arc volcanism.

4.1. Model limitations

Melt at the arc is produced in very little amount in the initial stages of the model as compared to the total melt amount produced later on. This is an artefact of the models due to the initial temperature field, in which the overriding plate has the same thickness everywhere. As the slab subducts, the corner flow brings hot mantle material at shallower depths, increasing the temperatures in the mantle wedge and enabling melt production. A uniformly hydrated mantle wedge and batch melting are assumed in these models, which is a simplification of the much more heterogeneous natural system. For instance, slab dehydration can occur at different depths and rates depending on

many factors, such as, but not only, mantle potential temperature, slab velocity, age, dip, and composition (Magni et al., 2014a; Van Keken et al., 2002). Fluids released from the slab can potentially focus into preferential channels and trigger mantle melting that would be heterogeneously distributed within the mantle wedge (Wilson et al., 2014). Moreover, when the mantle partially melts, fluids preferentially go into the melt and they are no longer available to hydrate the shallower part of the mantle wedge. Therefore, the estimates of wet melting production at the arc are likely overestimated in these models. This explains why no significant decrease of the amount of melt occurs when partially depleted mantle from the back-arc arrives at the mantle wedge.

By keeping track of the amount of depletion in the mantle and computing the melt accordingly, I take into account the composition of the residue and its potential to melt further. However, the fate of melt/fluids and the way they migrate are not explicitly modelled, as it goes beyond the scope of this work. Although this might affect the location and amount of melt at the small scale of the mantle wedge, it would likely not affect the large scale mantle flow and, thus, the results of this study.

4.2. Application to natural cases

The inflow of highly depleted material to the mantle wedge during slab retreat and back-arc spreading would most likely affect arc volcanism, both in terms of volcanic activity and magmatic composition. Indeed, there are many examples in present-day subduction zones where a gap in the volcanic activity at the arc corresponds to a period of active spreading in the back-arc region.

In the Izu-Bonin-Mariana (IBM) subduction zone, the extension in the overriding plate caused by slab roll-back produced two back-arc basins; the Shikoku Basin in the north (in the Izu-Bonin segment) and the Parece Vela Basin in the south (in the Mariana segment) (Lallemand, 2016). In both basins, spreading started at ∼29 Ma and ceased at ∼15 Ma (Takahashi et al., 2008; Taylor, 1992). Interestingly, this overlaps with a decrease in the volcanic activity at the arc started at 27 Ma and with a gap observed from the geologic record between 23-17 Ma in the Shikoku basin (Taylor, 1992). Similarly, in the Parece Vela Basin arc activity decreased at ∼30 Ma, ceased at ∼28 Ma, and resumed at 20 Ma (Taylor, 1992). These are in good agreement with my numerical models and with previous studies that also noticed that the period of less volcanic activity in the IBM subduction zone corresponds to the time of spreading in the Shikoku and Parece Vela Basins (e.g., Okino et al., 1998; Takahashi et al., 2008). Today the back-arc is not spreading in Izu-Bonin and the arc has been active for the past 17 Myr (Taylor, 1992). In the Mariana, the arc decreased its activity again at 9-5 Ma, but since then it has been active at the same time of the Mariana ridge spreading (<6 Ma) (Lallemand, 2016; Takahashi et al., 2008). However, at present, the Mariana slab is advancing (Heuret and Lallemand, 2005) and the mantle might flow differently than what described in the results of this study.

Between South of Japan and Taiwan, the Ryukyu Island arc and the Okinawa Trough in the back-arc are associated to the subduction of the Philippine Sea plate. The arc is mostly active in the northern part, where the back-arc is rifting and not spreading (e.g., Yan and Shi, 2014). In the south, instead, geochemical and petrological studies suggest that the back-arc might have started spreading <2 Ma (Yan and Shi, 2014). Interestingly, this seems to correspond to a relative minimum in the activity of the volcanic arc (Letouzey and Kimura, 1986). However, spreading of the southern part of the Okinawa Trough is still subject of debate, as some recent geophysical studies seem to suggest that the back-arc is now at a transitional phase between rifting and spreading (Arai et al., 2017). Other examples of phases of back-arc spreading associated with little or no volcanic activity are observed in the South Sandwich subduction zone (East Scotia Sea spreading <15 Ma, arc <8 Ma) (Leat et al., 2003), the Andaman Sea (spreading <5 Ma, arc <1 Ma) (Chakraborty and Khan, 2009), and the Tyrrhenian Sea (spreading 5-1 Ma, arc <1.5 Ma) (Rosenbaum et al., 2008). Uncertainties in the ages of arc activity and back-arc spreading can be quite large, especially considering that submarine arc remnants are not easy to find and identify as such, and they might be partially destroyed due to tectonic erosion processes at the trench (Lallemand, 2016). Therefore, important data that would give a more comprehensive view of the back-arc – arc magmatic evolution are currently lacking. Nonetheless, the tempo-spatial relationships between magmatism, mantle flow and trench behaviour described here may provide constraints for poorly understood paleo-subduction events deeper in the geological record, as well as improve regional plate tectonic models.

Other regions of the world do not conform to these temporal observations; for instance, the Lau Basin has been actively spreading since 4 Ma in the north and progressively opening southward (Bevis et al., 1995), and the arc does not reveal the expected gap in magmatic production. Rather, the volcanic arc has been active since at least 3 Ma (Turner and Hawkesworth, 1997). However, the composition of arc lavas show a very depleted source, especially in the north where slab retreat and spreading are faster (Turner and Hawkesworth, 1997). This depleted source could potentially come from the back-arc region, as suggested by Cooper et al. (2010). In the central and southern Lau Basin, things may be complicated by the fact that arc and back-arc are fairly close to each other and the anomalously high water content in the mantle wedge is thought to facilitate porous flow that connects the two plumbing systems, which are mixed in the upper mantle (Wei et al., 2015).

Even though the geometries of the presented models are clearly not representative of all subduction zones, the obtained tectonic evolution can be, at first order, used to better understand the many natural cases in which back-arc rifting or spreading are associated to trench retreat and increasing curvature, and/or slab rotation. Back-arc spreading rates obtained in this study (1-7 cm/yr) are within the range of those observed in present-day back-arcs that are actively spreading (0-13 cm/yr; Lallemand et al., 2005). Alternating phases of fast and slow spreading associated to slab windows formation, similar to the reference model (Section 3.1), are characteristic for example of the Tyrrhenian basin, in the Central Mediterranean (Magni et al., 2014b). The model presented in Section 3.4, in which extension of the overriding plate is larger towards the slab edge due to the strong rotation of the subducting plate, resembles the case of the Tonga subduction zone with the formation of the Lau basin. Although there is no large continental block entering the Tonga–Kermadec trench, the subduction of the Louisville seamount chain has been suggested to cause a similar style of rotation of the trench north of it (Wallace et al., 2009). Indeed, the Lau basin is spreading progressively faster northward, away from the pivot point of rotation (from 3 to 15 cm/yr (Bevis et al., 1995)) (Wallace et al., 2009), similar to the spreading rate pattern observed in my model (Fig. 6 and Fig. S1).

4.3. Toroidal flow

Results from this study show that different subducting plate geometries produce different mantle flow patterns. In particular, when toroidal mantle flow occurs around the slab edge, it has a much larger upwelling component than when the mantle flows through a slab window. In models in which the oceanic slab retreats faster in the middle of the subducting plate and slab windows form at the ocean-continent boundaries, the toroidal flow through these windows occurs at depths >200 km (Fig. 2). Passive tracers used to track the mantle flow stay at a similar depth throughout their entire journey from behind to the front of the

slab. Therefore, the mantle involved in the toroidal flow does not reach the arc and back-arc melting regions and does not affect their respective volcanism. On the other hand, when the oceanic slab is retreating faster at the side of the subducting plate, the mantle flows around the slab edge and it rises towards the surface (Fig. 6). In this case, the mantle that takes part in the toroidal flow reaches the surface and melts at the back-arc and/or at the arc. Part of the mantle also migrates into the narrow weak region that simulates a transform fault and melts through adiabatic decompression melting. This model prediction is in agreement with previous studies that found a similar pattern of toroidal mantle flow with a vertical component around slab edges (Crameri and Tackley, 2014; Király et al., 2017; Strak and Schellart, 2016). However, I do not observe the same upwelling component when the toroidal flow occurs through the slab window.

The reason for this difference is possibly two-fold. Firstly, the slab breaks off at about 200 km and although the tear propagates producing a larger window, the remnants of the detached slab prevent the mantle to flow at shallower depths. Therefore, the vertical extent of the toroidal flow cell is smaller than when the flow is around the slab edge and does not influence the corner flow produced by the ongoing subduction. Secondly, the rotation of the subducting plate is much larger in the case of the oceanic slab retreating at the side of the plate. This rotation creates a low pressure area in the arc and back-arc regions, enabling the upwelling component of the toroidal flow. Instead, in the slab window models, this upwelling does not occur, as the slab retreat at the centre of the plate is always trench perpendicular, which is a consequence of the symmetry of the model. If the formation of a slab window would occur only on one side or if slab windows would form at different times, it is reasonable to expect this asymmetry to produce some rotation of the oceanic subducting plate, thus, a change in the mantle flow. The investigation of the different types of toroidal mantle flow is not the main scope of this work and a more detailed study should be undertaken to explore this interesting mantle flow pattern variations and their tectonic and magmatic consequences.

5. Conclusions

In this study, I used 3D numerical models to investigate the interaction between arc and back-arc melts and the effects of mantle flow changes during subduction. The models show that as the back-arc is actively spreading and the slab is retreating a wide convection cell brings mantle from the back-arc to the sub-arc melting regions. Consequently, for ∼10-15 million years the source of arc melts is highly depleted mantle derived from the back-arc. A decrease or a break in the arc volcanic activity can therefore occur during back-arc spreading. After this phase, the classic corner flow driven by the downgoing slab is restored and fertile mantle is again the main source of melting in the mantle wedge above the slab. This is consistent with gaps in arc volcanism or with depleted mantle source of arc lavas in many present-day subduction zones with an actively spreading back-arc. Moreover, the toroidal mantle flow around the slab does not always rise towards the surface, but is likely to stay sub-horizontal at >200 km depth when it occurs through a newly formed slab window. Instead, when toroidal flow happens around the edge of a slab that is retreating and rotating, then this flow has a strong upwelling component that brings fertile mantle to the back-arc and sub-arc melting regions.

Acknowledgements

I would like to thank Pierre Bouilhol, Phil Heron, and Grace Shephard for their comments and suggestions on an early version of the manuscript. I would also like to thank Ryuta Arai and two anonymous reviewers for their constructive comments that helped improve the manuscript. This study was supported by the Research Council of Norway through its Centers of Excellence funding scheme, Project Number 223272 and made use of the UNINETT Sigma 2 computational resource allocation (Notur NN9283K and NorStore NS9029K).

Appendix A. Supplementary material

Supplementary material related to this article can be found online at https://doi.org/10.1016/j.epsl.2019.05.009.

References

Arai, R., Dunn, R.A., 2014. Seismological study of Lau back arc crust: mantle water, magmatic differentiation, and a compositionally zoned basin. Earth Planet. Sci. Lett. 390, 304–317.
Arai, R., Kodaira, S., Yuka, K., Takahashi, T., Miura, S., Kaneda, Y., 2017. Crustal structure of the southern Okinawa Trough: symmetrical rifting, submarine volcano, and potential mantle accretion in the continental back-arc basin. J. Geophys. Res., Solid Earth 122 (1), 622–641.
Arculus, R.J., Powell, R., 1986. Source component mixing in the regions of arc magma generation. J. Geophys. Res., Solid Earth 91, 5913–5926.
Bevis, M., Taylor, F.W., Schutz, B.E., Recy, J., Isacks, B.L., Helu, S., Singh, R., Kendrick, E., Stowell, J., Taylor, B., Calmantli, S., 1995. Geodetic observations of very rapid convergence and back-arc extension at the Tonga arc. Nature 374, 249.
Byerlee, J.P., 1978. Friction of rocks. Pure Appl. Geophys. 116, 615–626.
Chakraborty, P.P., Khan, P.K., 2009. Cenozoic geodynamic evolution of the Andaman–Sumatra subduction margin: current understanding. Isl. Arc 18, 184–200.
Cooper, L.B., Plank, T., Arculus, R.J., Hauri, E.H., Hall, P.S., Parman, S.W., 2010. High-Ca boninites from the active Tonga Arc. J. Geophys. Res., Solid Earth 115.
Crameri, F., Tackley, P.J., 2014. Spontaneous development of arcuate single-sided subduction in global 3-D mantle convection models with a free surface. J. Geophys. Res., Solid Earth 119, 5921–5942.
Ducea, M.N., Saleeby, J.B., Bergantz, G., 2015. The architecture, chemistry, and evolution of continental magmatic arcs. Annu. Rev. Earth Planet. Sci. 43, 299–331.
Faccenna, C., Civetta, L., D'Antonio, M., Funiciello, F., Margheriti, L., Piromallo, C., 2005. Constraints on mantle circulation around the deforming Calabrian slab. Geophys. Res. Lett. 32.
Govers, R., Wortel, M.J.R., 2005. Lithosphere tearing at STEP faults: response to edges of subduction zones. Earth Planet. Sci. Lett. 236, 505–523.
Hall, P.S., Cooper, L.B., Plank, T., 2012. Thermochemical evolution of the sub-arc mantle due to back-arc spreading. J. Geophys. Res., Solid Earth 117.
Harmon, N., Blackman, D.K., 2010. Effects of plate boundary geometry and kinematics on mantle melting beneath the back-arc spreading centers along the Lau Basin. Earth Planet. Sci. Lett. 298 (3–4), 334–346.
Hashima, A., Fukahata, Y., Matsu'ura, M., 2008. 3-D simulation of tectonic evolution of the Mariana arc–back-arc system with a coupled model of plate subduction and back-arc spreading. Tectonophysics 458 (1–4), 127–136.
Hawkins, J., Melchior, J., 1985. Petrology of Mariana Trough and Lau basin basalts. J. Geophys. Res., Solid Earth 90, 11431–11468.
Heuret, A., Lallemand, S., 2005. Plate motions, slab dynamics and back-arc deformation. Phys. Earth Planet. Inter. 149, 31–51.
Hirth, G., Kohlstedt, D., 2003. Rheology of the upper mantle and the mantle wedge: a view from the experimentalists. In: Inside the Subduction Factory, pp. 83–105.
Katz, R.F., Spiegelman, M., Langmuir, C.H., 2003. A new parameterization of hydrous mantle melting. Geochem. Geophys. Geosyst. 4.
Kelemen, P., Hirth, G., Shimizu, N., Spiegelman, M., Dick, H., 1997. A review of melt migration processes in the adiabatically upwelling mantle beneath oceanic spreading ridges. Philos. Trans. R. Soc. Lond. A, Math. Phys. Eng. Sci. 355, 283–318.
Kelley, K.A., Plank, T., Grove, T.L., Stolper, E.M., Newman, S., Hauri, E., 2006. Mantle melting as a function of water content beneath back-arc basins. J. Geophys. Res., Solid Earth 111.
Király, Á., Capitanio, F.A., Funiciello, F., Faccenna, C., 2017. Subduction induced mantle flow: length-scales and orientation of the toroidal cell. Earth Planet. Sci. Lett. 479, 284–297.
Korenaga, J., Karato, S.-I., 2008. A new analysis of experimental data on olivine rheology. J. Geophys. Res., Solid Earth 113.
Lallemand, S., 2016. Philippine Sea Plate inception, evolution, and consumption with special emphasis on the early stages of Izu-Bonin-Mariana subduction. Prog. Earth Planet. Sci. 3, 15.
Lallemand, S., Heuret, A., Boutelier, D., 2005. On the relationships between slab dip, back-arc stress, upper plate absolute motion, and crustal nature in subduction zones. Geochem. Geophys. Geosyst. 6 (9).
Langmuir, C., Bezos, A., Escrig, S., Parman, S., 2006. Chemical systematics and hydrous melting of the mantle in back-arc basins. In: Back-Arc Spreading Systems: Geological, Biological, Chemical, and Physical Interactions, pp. 87–146.

Leat, P., Smellie, J., Millar, I., Larter, R., 2003. Magmatism in the South Sandwich Arc. Special Publications, vol. 219. Geological Society, London, pp. 285–313.
Letouzey, J., Kimura, M., 1986. The Okinawa Trough: genesis of a back-arc basin developing along a continental margin. Tectonophysics 125, 209–230.
Magni, V., Bouilhol, P., van Hunen, J., 2014a. Deep water recycling through time. Geochem. Geophys. Geosyst. 15, 4203–4216.
Magni, V., Faccenna, C., van Hunen, J., Funiciello, F., 2014b. How collision triggers backarc extension: insight into Mediterranean style of extension from 3-D numerical models. Geology 42, 511–514.
McKenzie, D.P., 1969. Speculations on the consequences and causes of plate motions. Geophys. J. Int. 18, 1–32.
Moresi, L., Betts, P.G., Miller, M.S., Cayley, R.A., 2014. Dynamics of continental accretion. Nature 508 (7495), 245.
Moresi, L., Gurnis, M., 1996. Constraints on the lateral strength of slabs from three-dimensional dynamic flow models. Earth Planet. Sci. Lett. 138, 15–28.
Okino, K., Kasuga, S., Ohara, Y., 1998. A new scenario of the Parece Vela Basin genesis. Mar. Geophys. Res. 20, 21–40.
Pearce, J.A., Peate, D.W., 1995. Tectonic implications of the composition of volcanic arc magmas. Annu. Rev. Earth Planet. Sci. 23, 251–285.
Pearce, J.A., Stern, R.J., 2006. Origin of back-arc basin magmas: trace element and isotope perspectives. In: Back-Arc Spreading Systems: Geological, Biological, Chemical, and Physical Interactions, pp. 63–86.
Ringwood, A.E., 1974. The petrological evolution of island arc systems: twenty-seventh William Smith Lecture. J. Geol. Soc. 130, 183–204.
Rosenbaum, G., Gasparon, M., Lucente, F.P., Peccerillo, A., Miller, M.S., 2008. Kinematics of slab tear faults during subduction segmentation and implications for Italian magmatism. Tectonics 27.
Sobolev, A.V., Chaussidon, M., 1996. H_2O concentrations in primary melts from supra-subduction zones and mid-ocean ridges: implications for H_2O storage and recycling in the mantle. Earth Planet. Sci. Lett. 137, 45–55.
Strak, V., Schellart, W.P., 2016. Control of slab width on subduction-induced upper mantle flow and associated upwellings: insights from analog models. J. Geophys. Res., Solid Earth 121, 4641–4654.
Takahashi, N., Kodaira, S., Tatsumi, Y., Kaneda, Y., Suyehiro, K., 2008. Structure and growth of the Izu-Bonin-Mariana arc crust: 1. Seismic constraint on crust and mantle structure of the Mariana arc–back-arc system. J. Geophys. Res., Solid Earth 113.
Taylor, B., 1992. Rifting and the volcanic-tectonic evolution of the Izu-Bonin-Mariana arc. In: Proceedings of Ocean Drilling Program, Scientific Results, vol. 126. Ocean Drilling Program, College Station, TX, USA, pp. 625–651.
Turcotte, D.L., Schubert, G., 2002. Plate tectonics. In: Geodynamics, 2nd edn. Cambridge University Press, Cambridge/New York, pp. 1–21.
Turner, S., Hawkesworth, C., 1997. Constraints on flux rates and mantle dynamics beneath island arcs from Tonga–Kermadec lava geochemistry. Nature 389, 568.
Uyeda, S., Kanamori, H., 1979. Back-arc opening and the mode of subduction. J. Geophys. Res., Solid Earth 84, 1049–1061.
Van Keken, P.E., Kiefer, B., Peacock, S.M., 2002. High-resolution models of subduction zones: implications for mineral dehydration reactions and the transport of water into the deep mantle. Geochem. Geophys. Geosyst. 3, 20 pp.
Wallace, L.M., Ellis, S., Mann, P., 2009. Collisional model for rapid fore-arc block rotations, arc curvature, and episodic back-arc rifting in subduction settings. Geochem. Geophys. Geosyst. 10.
Wei, S.S., Wiens, D.A., Zha, Y., Plank, T., Webb, S.C., Blackman, D.K., et al., 2015. Seismic evidence of effects of water on melt transport in the Lau back-arc mantle. Nature 518 (7539), 395.
Wilson, C.R., Spiegelman, M., van Keken, P.E., Hacker, B.R., 2014. Fluid flow in subduction zones: the role of solid rheology and compaction pressure. Earth Planet. Sci. Lett. 401, 261–274.
Woodhead, J., Eggins, S., Gamble, J., 1993. High field strength and transition element systematics in island arc and back-arc basin basalts: evidence for multi-phase melt extraction and a depleted mantle wedge. Earth Planet. Sci. Lett. 114, 491–504.
Yan, Q., Shi, X., 2014. Petrologic perspectives on tectonic evolution of a nascent basin (Okinawa Trough) behind Ryukyu Arc: a review. Acta Oceanol. Sin. 33, 1–12.